Pramana – J. Phys. (2019) 92:52
https://doi.org/10.1007/s12043-018-1712-0

Synchronisation of integer-order and fractional-order discrete-time chaotic systems

ADEL OUANNAS[1], AMINA-AICHA KHENNAOUI[2], OKBA ZEHROUR[2], SAMIR BENDOUKHA[3], GIUSEPPE GRASSI[4] and VIET-THANH PHAM[5,*]

[1]Mathematics and Computer Science Department, Tebessa University, 12062 Tebessa, Algeria
[2]Department of Mathematics and Computer Sciences, University of Larbi Ben M'hidi, Oum El Bouaghi, Algeria
[3]Department of Electrical Engineering, College of Engineering, Yanbu, Taibah University, Medina, Saudi Arabia
[4]Dipartimento Ingegneria Innovazione, Universita del Salento, 73100 Lecce, Italy
[5]Nonlinear Systems and Applications, Faculty of Electrical & Electronics Engineering, Ton Duc Thang University, Ho Chi Minh City, Vietnam
*Corresponding author. E-mail: phamvietthanh@tdtu.edu.vn

MS received 21 June 2018; revised 23 August 2018; accepted 29 August 2018; published online 15 February 2019

Abstract. This paper studies the synchronisation of integer- and fractional-order discrete-time chaotic systems with different dimensions. Control laws are proposed for the full-state hybrid projective synchronisation (FSHPS) of a master–slave pair, where the difference equations of the master have an integer order while those of the slave have a fractional order. Moreover, inverse FSHPS laws are proposed for a fractional-order master and an integer-order slave. The Lyapunov stability theory of integer-order maps and the stability theory of linear fractional-order maps are utilised to establish the asymptotic stability of the zero equilibrium corresponding to the synchronisation error system. Numerical results are presented to verify the findings of the study.

Keywords. Full-state hybrid projective synchronisation; inverse full-state hybrid projective synchronisation; chaotic maps; fractional discrete-time systems; Lyapunov stability.

PACS Nos 05.45.−a; 05.45.Xt

1. Introduction

Chaotic dynamical systems have been shown to emerge from natural phenomena such as the weather or from designed engineering problems such as the movement of a rigid body in three-dimensional (3D) space. These systems possess different beneficial properties including their random-like trajectories and high sensitivity to initial conditions. Interest in this type of systems grew exponentially once it became clear that the synchronisation of two chaotic systems is feasible. This means that chaotic systems may be controlled and their path is determined, which highlighted the benefits of the random-like behaviour. Since the pioneering work of Pecora and Carrol [1], in which they demonstrated chaos synchronisation, thousands of articles have been published all around the globe. The topics covered by the vast amount of literature include types of synchronisation and the corresponding adaptive control strategies as well as the application of chaos and synchronisation in the fields of science and engineering.

Perhaps the most talked about application is in the field of secure communications [2]. In order to achieve secure communication, chaos can be employed in a number of stages. It can be used at the physical layer, either to mask the transmitted message [3,4], as a modulation carrier [5,6], or to provide multiple access to the transmission medium [7]. Alternatively, chaos may be used to produce a map based on which data encryption is carried out. Whether secret key or public key encryption is adopted, a set of random keys is required and this is where chaos comes in handy. However, instead of continuous-time chaotic systems, their discrete counterpart is required [8]. At the receiver side, the encryption keys must be reproduced by means of synchronisation, see [9]. This, along with many more applications available for the synchronisation of discrete-time chaotic systems, has motivated many to do research in this subject. Several discrete-time chaotic systems have

been proposed in the literature [10–13] and numerous studies have investigated synchronisation types and control strategies [14–19]. All these studies consider the addition of an adaptive term to the states of the dynamical system to force a specific trajectory. Studies have shown that the synchronisation of two systems is highly dependent on the initial setting and that by resetting the initial values, one can control the states of the system [20].

In recent years, fractional discrete-time calculus has become somewhat of a hot topic. A few researchers have attempted to develop a framework for the subject and investigate the stability and application of fractional discrete-time chaotic system [21–25]. Some conventional discrete-time maps have been extended to the fractional case [26–28]. The synchronisation and application of these types of systems remain mostly unexplored to this day. A few studies can be found in [29–34]. Moreover, to the best of the knowledge of the authors, no studies can be found that attempt the synchronisation of a mixed pair of integer-order and fractional-order systems as is the case with continuous-time systems (see [35,36]). This has motivated the authors of this work to investigate the possibility of synchronising two systems with integer and fractional orders. In our study, we consider two types of synchronisation, namely the full-state hybrid projective synchronisation (FSHPS) [37] and the inverse FSHPS (IFSHPS) [18]. A detailed description of these synchronisations will be shown in the following two sections along with the proposed control laws and the proofs of their convergence. Also, numerical examples are used to illustrate the validity of the proposed synchronisation schemes.

2. FSHPS between integer master and fractional slave maps

In order to establish the synchronisation strategy between an integer-order master and a fractional-order slave maps, we consider the pair of discrete-time systems given by

$$\begin{cases} {}^{\mathrm{C}}\Delta^{\alpha} X(t) = f(X(t+\alpha-1)), & t \in \mathbb{N}_{a+\alpha-1}, \\ Y(t+1) = BY(t) + g(Y(t)) + U, & t \in \mathbb{N}, \end{cases} \tag{1}$$

where $X(t) = (x_1(t), \ldots, x_n(t))^{\mathrm{T}}$ and $Y(t) = (y_1(t), \ldots, y_m(t))^{\mathrm{T}}$ represent the states of the master and slave systems, respectively, $f: \mathbb{R}^n \longrightarrow \mathbb{R}^n$, $B = (b_{ij})_{m\times m}$, $g: \mathbb{R}^m \longrightarrow \mathbb{R}^m$ is a vector of nonlinear function and $U = (u_i)_{1\le i\le m}$ are control parameters to be identified by means of the synchronisation strategy. Note that the master map is a fractional one with difference order α, whereas the slave is an integer-order map with linear and nonlinear parts.

The notation ${}^{\mathrm{C}}\Delta_a^{\alpha} X(t)$ denotes the α-Caputo-type delta difference of the function $X(t): \mathbb{N}_a \to \mathbb{R}$ with $\mathbb{N}_a = \{a, a+1, a+2, \ldots\}$ [22], which is of the form

$$\begin{aligned} {}^{\mathrm{C}}\Delta_a^{\alpha} X(t) &= \Delta_a^{-(n-\alpha)} \Delta^n X(t) \\ &= \frac{1}{\Gamma(n-\alpha)} \sum_{s=a}^{t-(n-\alpha)} (t-s-1)^{(n-\alpha-1)} \\ &\quad \times \Delta^n X(s), \end{aligned} \tag{2}$$

for $\alpha \notin \mathbb{N}$ is the fractional order, $t \in \mathbb{N}_{a+n-\alpha}$ and $n = \lceil \alpha \rceil + 1$. In (2), the αth fractional sum $\Delta_a^{-\alpha} X(t)$ is defined similar to [21] as

$$\Delta_a^{-\alpha} X(t) = \frac{1}{\Gamma(\alpha)} \sum_{s=a}^{t-\alpha} (t-s-1)^{(\alpha-1)} X(s) \tag{3}$$

with $\alpha > 0$ and $t \in \mathbb{N}_{a+\alpha}$. The term $t^{(\alpha)}$ denotes the falling function defined in terms of the Gamma function Γ as

$$t^{(\alpha)} = \frac{\Gamma(t+1)}{\Gamma(t+1-\alpha)}. \tag{4}$$

Note that the subscript a is dropped in (1) and throughout this paper as we assume $a = 0$.

Let us now define what is meant by FSHPS and present the first theorem of this paper.

DEFINITION 1

The fractional-order master map and the integer-order slave map described by (1) are said to be FSHP-synchronised if there exists a controller U and a constant matrix $\theta = (\theta_{ij})_{m\times n}$ such that the synchronisation errors

$$e_i(t) = y_i(t) - \sum_{j=1}^{n} \theta_{ij} x_j(t), \quad i = 1, 2, \ldots, m, \quad t \in \mathbb{N} \tag{5}$$

satisfy the asymptotic rule

$$\lim_{t\to\infty} e_i(t) = 0, \quad i = 1, 2, \ldots, m. \tag{6}$$

Theorem 1. *The master and slave maps in* (1) *are FSHP-synchronised if*

$$U = (B - C)\, e(t) - BY(t) - g\,(Y(t)) + \theta X(t+1), \tag{7}$$

where $C \in \mathbb{R}^{m\times m}$ *is a control matrix satisfying the condition that matrix*

$$(B-C)^{\mathrm{T}}(B-C)-I \tag{8}$$

is negative definite.

Proof. From (5), we have

$$e_i(t+1) = y_i(t+1) - \sum_{j=1}^{n}\theta_{ij}x_j(t+1), \quad i = 1,\ldots,m \tag{9}$$

can be described more compactly as

$$e(t+1) = BY(t) + g(Y(t)) + U - \theta X(t+1). \tag{10}$$

After using the control law (7), the error system (10) yields the simplified system

$$e(t+1) = (B-C)\,e(t). \tag{11}$$

The resulting system (11) is integer order and thus its stability is classical. As a result, by using the Lyapunov function $V(e(t)) = e^{\mathrm{T}}(t)e(t)$, we have

$$\begin{aligned}\Delta V(e(t)) &= e^{\mathrm{T}}(t+1)e(t+1) - e^{\mathrm{T}}(t)e(t)\\ &= e^{\mathrm{T}}(t)(B-C)^{\mathrm{T}}(B-C)e(t)\\ &\quad - e^{\mathrm{T}}(t)e(t)\\ &= e^{\mathrm{T}}(t)[(B-C)^{\mathrm{T}}(B-C)-I]e(t).\end{aligned}$$

Since $(B-C)^{\mathrm{T}}(B-C)-I$ is negative definite, it simply follows that

$$\Delta V(e(t)) \le 0$$

and by integer-order Lyapunov stability theory, we have

$$\lim_{t\longrightarrow+\infty} e_i(t) = 0, \quad i = 1,2,\ldots,m.$$

Hence, by Definition 1, pair (1) is FSHP-synchronised. □

In order to verify the result of Theorem 1, let us take the following example.

Example 1. Consider as master the two-dimensional (2D) fractional Hénon map proposed in [26] and given by

$$\begin{cases} {}^{\mathrm{C}}\Delta^{\alpha}x_1(t) = x_2(t+\beta-1)\\ \qquad\qquad +1 - a_1x_1^2(t+\beta-1) - x_1(t+\beta-1),\\ {}^{\mathrm{C}}\Delta^{\alpha}x_2(t) = b_1x_1(t+\beta-1)\\ \qquad\qquad -x_2(t+\beta-1), \quad t\in\mathbb{N}_{\alpha-1}.\end{cases} \tag{12}$$

This map has been shown to have a chaotic attractor for specific values of parameters such as $(a_1, b_1) = (1.4,\ 0.3)$ and $\alpha = 0.984$. The phase portrait of this particular example is depicted in figure 1 for $x_1(0) = x_2(0) = 0$. As for the slave map, we consider the 3D integer-order generalised Hénon map proposed in [12]. The slave map is of the form

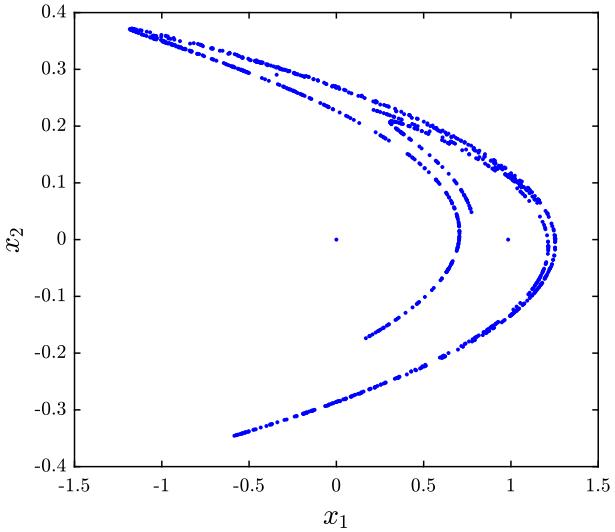

Figure 1. Phase-space plot for the fractional Hénon map with $(a_1,\ b_1) = (1.4,\ 0.3)$, $\alpha = 0.984$ and $x_1(0) = x_2(0) = 0$.

$$\begin{cases} y_1(t+1) = -b_2y_3(t) + u_1,\\ y_2(t+1) = b_2y_3(t) + y_1(t) + u_2,\\ y_3(t+1) = 1 + y_2(t) - a_2y_3^2(t) + u_3,\end{cases} \tag{13}$$

where $u_1(t), u_2(t)$ and $u_3(t)$ are controllers. This map has been studied by many researchers and applied in different applications. For $u_1(t) = u_2(t) = u_3(t) = 0$, it exhibits a chaotic behaviour, for instance, when $(a_2, b_2) = (1.07, 0.3)$. This behaviour is depicted in figure 2 for initial conditions $(y_1(0), y_2(0), y_3(0)) = (0.1, 0.2, 0.5)$.

The linear part of the slave is given by

$$B = \begin{pmatrix} 0 & 0 & -b_2\\ 1 & 0 & b_2\\ 0 & 1 & 0\end{pmatrix}. \tag{14}$$

We aim to determine the controllers $u_i, i = 1, 2, 3$, that will drive the slave map (13) to synchronise with the master map (12) under Definition 1. We start by formulating the error system (10)

$$\begin{aligned}(e_1(t), e_2(t), e_3(t))^{\mathrm{T}} &= (y_1(t), y_2(t), y_3(t))^{\mathrm{T}}\\ &\quad - \theta\times(x_1(t), x_2(t))^{\mathrm{T}},\end{aligned} \tag{15}$$

where

$$\theta = (\theta_{ij}) = \begin{pmatrix} 1 & 2\\ 0 & 3\\ -1 & 1\end{pmatrix}. \tag{16}$$

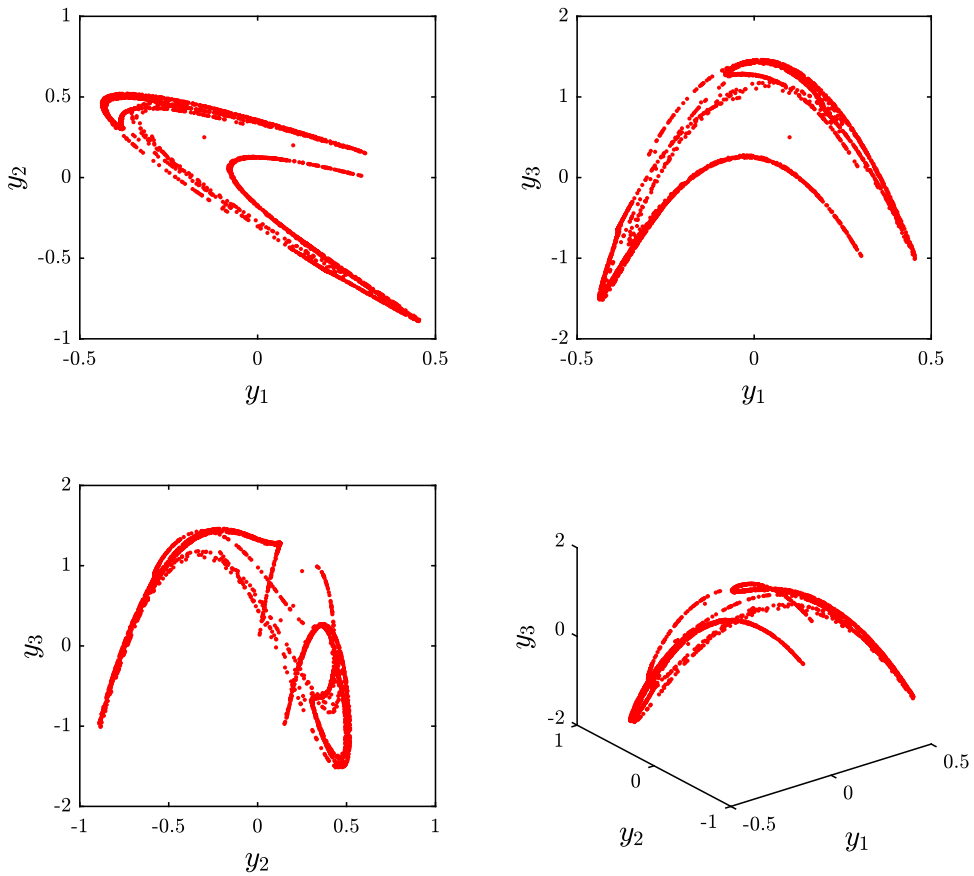

Figure 2. Phase portraits for the generalised 3D Hénon map with $(a_2,\ b_2) = (1.07, 0.3)$ and $(y_1(0), y_2(0), y_3(0)) = (0.1, 0.2, 0.5)$.

Next, according to Theorem 1, we find a suitable control matrix C such that $(B - C)^{\mathrm{T}}(B - C) - I$ is negative definite. It can be easily verified that

$$C = \begin{pmatrix} \frac{-1}{\sqrt{6}} & \frac{-1}{2} & -b_2 - \frac{1}{2\sqrt{3}} \\ 1 + \frac{1}{\sqrt{6}} & \frac{-1}{2} & b_2 - \frac{1}{2\sqrt{3}} \\ \frac{-1}{\sqrt{6}} & 1 & -\frac{1}{\sqrt{3}} \end{pmatrix} \tag{17}$$

is sufficient. The last step is to calculate the control vector $U = (u_i)_{1\le i\le 3}$ according to (7) and use it to drive the slave map. The resulting error system is given by

$$\begin{cases} e_1(t+1) = \frac{1}{\sqrt{6}}e_1(t) + \frac{1}{2}e_2(t) - \frac{1}{2\sqrt{3}}e_3(t), \\ e_2(t+1) = \frac{-1}{\sqrt{6}}e_1(t) + \frac{1}{2}e_2(t) + \frac{1}{2\sqrt{3}}e_3(t), \\ e_3(t+1) = \frac{1}{\sqrt{6}}e_1(t) + \frac{1}{\sqrt{3}}e_3(t). \end{cases} \tag{18}$$

Figure 3 depicts the time evolution of the errors (18) with initial states $(e_1(0), e_2(0), e_3(0)) = (0.57, 0.57, 0.57)$. Clearly, the errors decay to zero in sufficient time, which means that the master and the slave maps (12) and (13) are synchronised.

Usually, when dealing with continuous- or discrete-time systems, the computational complexity is an important aspect. For continuous-time chaotic systems that represent the dynamics of a nonlinear circuit, complexity can be estimated via integration in a transient period or similar to [38]. However, in discrete-time systems, such an approach is not applicable. One may assess the complexity of the proposed control rule (7) in terms of the number of multiply accumulate (MAC) operations required for a single iteration of the controller. Since the number of MACs is dependent on the nonlinear function g, it may not be estimated in the general case. For the example at hand, we have

$$g(Y(t)) = \begin{pmatrix} 0 \\ 0 \\ 1 - a_2 y_3^2(t) \end{pmatrix}. \tag{19}$$

Hence, the number of MACs required to evaluate one iteration of (7) is $2m^2 + mn + 5 = 29$.

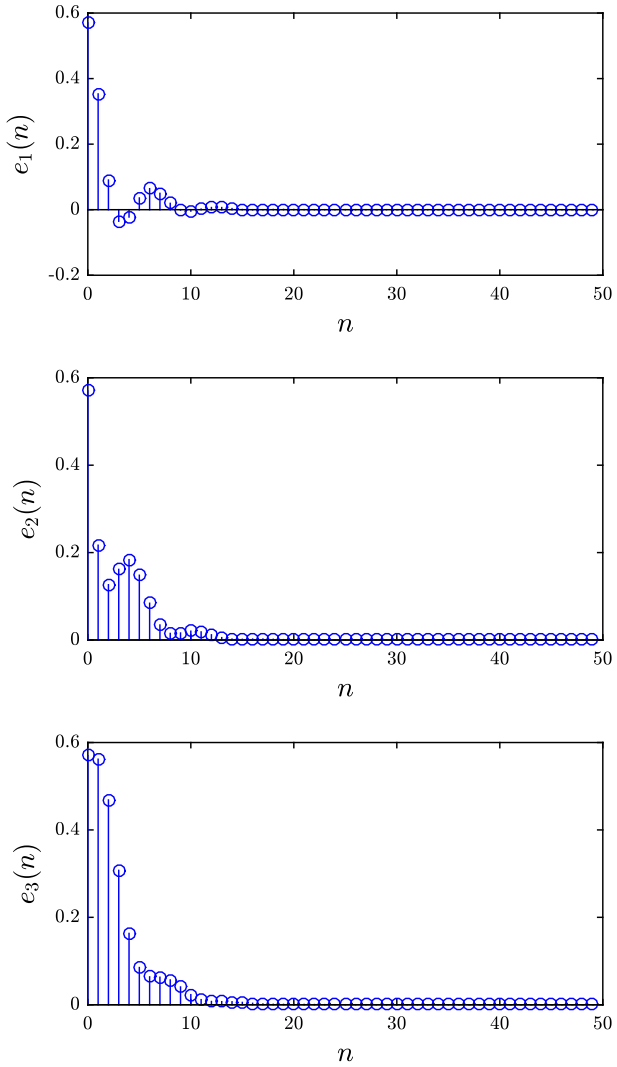

Figure 3. The evolution of errors over time for the first example as in (18).

3. IFSHPS between fractional master and integer slave maps

We now look at the synchronisation of a fractional-order master map and an integer-order slave map. Consider the pair

$$\begin{cases} X(t+1) = f(X(t)), \quad t \in \mathbb{N}, \\ {}^{C}\Delta^{\beta} Y(t) = BY(t+\beta-1) + g(Y(t+\beta-1)) \\ \qquad\qquad +U(t+\beta-1), \quad t \in \mathbb{N}_{\beta-1}, \end{cases} \tag{20}$$

where $X(t) = (x_1(t), \ldots, x_n(t))^{\mathrm{T}}$ and $Y(t) = (y_1(t), \ldots, y_m(t))^{\mathrm{T}}$ are the master and the slave state vectors, respectively, $f: \mathbb{R}^n \longrightarrow \mathbb{R}^n$, $B = (b_{ij})_{m\times m}$, $g: \mathbb{R}^m \longrightarrow \mathbb{R}^m$ is a nonlinear function and $U = (u_i)_{1\le i\le m}$ is a control vector. In this case, we assume that $n < m$. The following definition describes the type of synchronisation considered in this section.

DEFINITION 2

The master–slave pair (20) is said to be inverse IFSHPS if there exists a control vector U and a scaling constant matrix $\gamma = (\gamma_{ij})_{n\times m}$ such that the synchronisation errors

$$\lim_{t\to\infty} \left| e_i(t) := x_i(t) - \sum_{j=1}^{m} \gamma_{ij} y_j(t) \right| = 0, \tag{21}$$

for $i = 1, 2, \ldots, n$.

In order to establish the asymptotic stability of the control law described below, we require fractional stability methods. Let us start by stating the following theorem related to the linear stability of fractional maps.

Theorem 2 [39]. *The zero equilibrium of the linear fractional-order discrete-time system*

$${}^{C}\Delta_a^{\upsilon} e(t) = \mathbf{D} e(t+\upsilon-1), \tag{22}$$

where $e(t) = (e_1(t), \ldots, e_n(t))^{\mathrm{T}}$, $0 < \upsilon \le 1$, $\mathbf{D} \in \mathbb{R}^{n\times n}$ *and* $\forall t \in \mathbb{N}_{a+1-\upsilon}$, *is asymptotically stable if*

$$\lambda \in \left\{ z \in \mathbb{C}: \ |z| < \left(2\cos \frac{|\arg z| - \pi}{2-\upsilon} \right)^{\upsilon} \right.$$

and

$$\left. |\arg z| > \frac{\upsilon\pi}{2} \right\} \tag{23}$$

for all the eigenvalues λ *of* $\mathbf{D}$.

In order to achieve IFSHPS, we take the following fractional difference equation of the error vector $e(t) = (e_1(t), \ldots, e_n(t))^{\mathrm{T}}$ yielding

$$\begin{aligned} {}^{C}\Delta^{\beta} e(t) = {}& {}^{C}\Delta^{\beta} X(t) - \gamma B Y(t+\beta-1) \\ & -\gamma g(Y(t+\beta-1)) - \gamma U. \end{aligned} \tag{24}$$

For simplicity, we append the control vector U with zeros for $i > n$, i.e.

$$u_i = 0, \quad i = n+1, n+2, \ldots, m. \tag{25}$$

Using (25), the error system (24) simplifies to

$${}^{C}\Delta^{\beta} e(t) = R - \hat{\gamma}\hat{U}, \tag{26}$$

where

$$\begin{aligned} R = {}& {}^{C}\Delta^{\beta} X(t) - \gamma B Y(t+\beta-1) \\ & - \gamma g(Y(t+\beta-1)), \end{aligned} \tag{27}$$

and $\hat{U} = (u_1, \ldots, u_n)^{\mathrm{T}}$ and $\hat{\gamma} = (\gamma_{ij})_{n\times n}$ is assumed to be an $n \times n$ invertible matrix with its inverse being denoted by $\hat{\gamma}^{-1}$.

In order to achieve IFSHPS between maps (20), we may choose the vector controller $\hat{U} = (u_1, \ldots, u_n)^{\mathrm{T}}$ as follows:

$$\hat{U} = \hat{\gamma}^{-1}[(L - \hat{B})\,(X(t) - \gamma Y(t)) + R], \tag{28}$$

where $\hat{B} = (b_{ij})_{n\times n}$ and $L \in \mathbb{R}^{n\times n}$ is an appropriate control matrix selected such that all the eigenvalues of $\hat{B} - L$ satisfy

$$-2^{\beta} < \lambda_i < 0, \quad i = 1, 2, \ldots, n. \tag{29}$$

Substituting (28) into (26) yields the new error dynamics

$${}^{\mathrm{C}}\Delta^{\beta} e(t) = (\hat{B} - L)e(t + \beta - 1). \tag{30}$$

In order to show that the zero solution of (30) is globally asymptotically stable, we use the stability theory of linear fractional-order maps as described in Theorem 2. According to condition (29), it is easy to see that all the eigenvalues of the matrix $\hat{B} - L$ satisfy

$$|\arg \lambda_i| = \pi > \frac{\beta\pi}{2}$$

and

$$|\lambda_i| < \left(2\cos\frac{|\arg\lambda_i| - \pi}{2 - \beta}\right)^{\beta}, \tag{31}$$

for $i = 1, 2, \ldots, n$. Hence, using Theorem 2, the zero solution of (30) is globally asymptotically stable and the master–slave pair (20) is IFSHP-synchronised. The following theorem summarises the control strategy. A numerical example is also provided to illustrate the control strategy described therein.

Theorem 3. *The master and the slave pair* (20) *are IFSHP-synchronised subject to a matrix L being selected such that all the eigenvalues of* $(\hat{B} - L)$ *satisfy* (31) *and control vector U being chosen as described in* (25) *and* (28).

Example 2. In order to put Theorem 3 to the test, let us consider as master the 2D Hénon map [10] described by

$$\begin{cases} x_1(t+1) = x_2(t) + 1 - a_1 x_1^2(t), \\ x_2(t+1) = b_1 x_1(t). \end{cases} \tag{32}$$

This map is well known and has a chaotic attractor, for example, when $(a_1, b_1) = (1.4, 0.3)$. This chaotic behaviour is shown in figure 4 for initial conditions $x_1(0) = x_2(0) = 0$. As for the slave map, we consider the fractional generalised 3D Hénon map proposed in [27] and given by

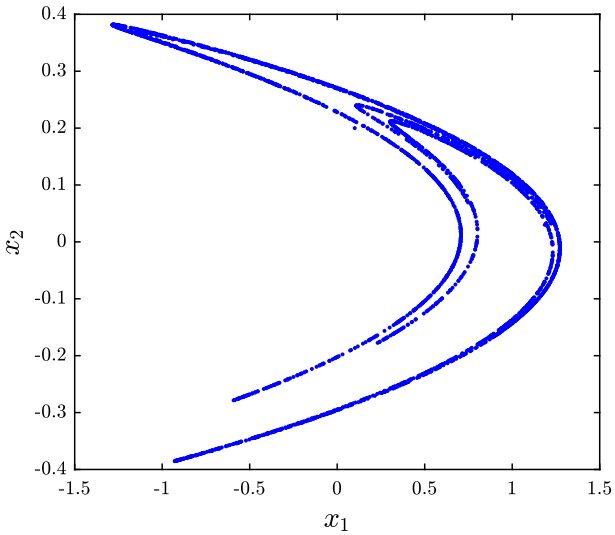

Figure 4. Phase-space plot for the integer-order Hénon map with $(a_1, b_1) = (1.4, 0.3)$ and $x_1(0) = x_2(0) = 0$.

$$\begin{cases} {}^{\mathrm{C}}\Delta^{\beta} y_1(t) = -y_1(t+\beta-1) - b_2 y_3(t+\beta-1) \\ \qquad\qquad +u_1(t+\beta-1), \\ {}^{\mathrm{C}}\Delta^{\beta} y_2(t) = b_2 y_3(t+\beta-1) + y_1(t+\beta-1) \\ \qquad\qquad -y_2(t+\beta-1) + u_2(t+\beta-1), \\ {}^{\mathrm{C}}\Delta^{\beta} y_3(t) = 1 + y_2(t+\beta-1) - a_2 y_3^2(t+\beta-1) \\ \qquad\qquad -y_3(t+\beta-1) + u_3(t+\beta-1). \end{cases} \tag{33}$$

It was shown in [27] that for $(a_2, b_2) = (0.99, 0.2)$ and $\beta = 0.984$, the map (33) with $u_1 = u_2 = u_3 = 0$ is chaotic. Given initial states $(y_1(0), y_2(0), y_3(0)) = (0.1, 0.2, 0.5)$, the phase-space plots are depicted in figure 5. The linear part of the slave map can be written in matrix form as

$$B = \begin{pmatrix} -1 & 0 & -b_2 \\ 1 & -1 & b_2 \\ 0 & 1 & -1 \end{pmatrix}. \tag{34}$$

So, the matrix $\hat{B}$ is given by

$$\hat{B} = \begin{pmatrix} -1 & 0 \\ 1 & -1 \end{pmatrix}. \tag{35}$$

We start by defining the synchronisation errors (21) as

$$(e_1(t), e_2(t))^{\mathrm{T}} = (x_1(t), x_2(t))^{\mathrm{T}} - \gamma \times (y_1(t), y_2(t), y_3(t))^{\mathrm{T}}, \tag{36}$$

where

$$\gamma = (\gamma_{ij}) = \begin{pmatrix} 2 & 0 & 4 \\ 0 & 3 & 1 \end{pmatrix}. \tag{37}$$

In order to find the suitable controls (28), we must first take the reduced matrix

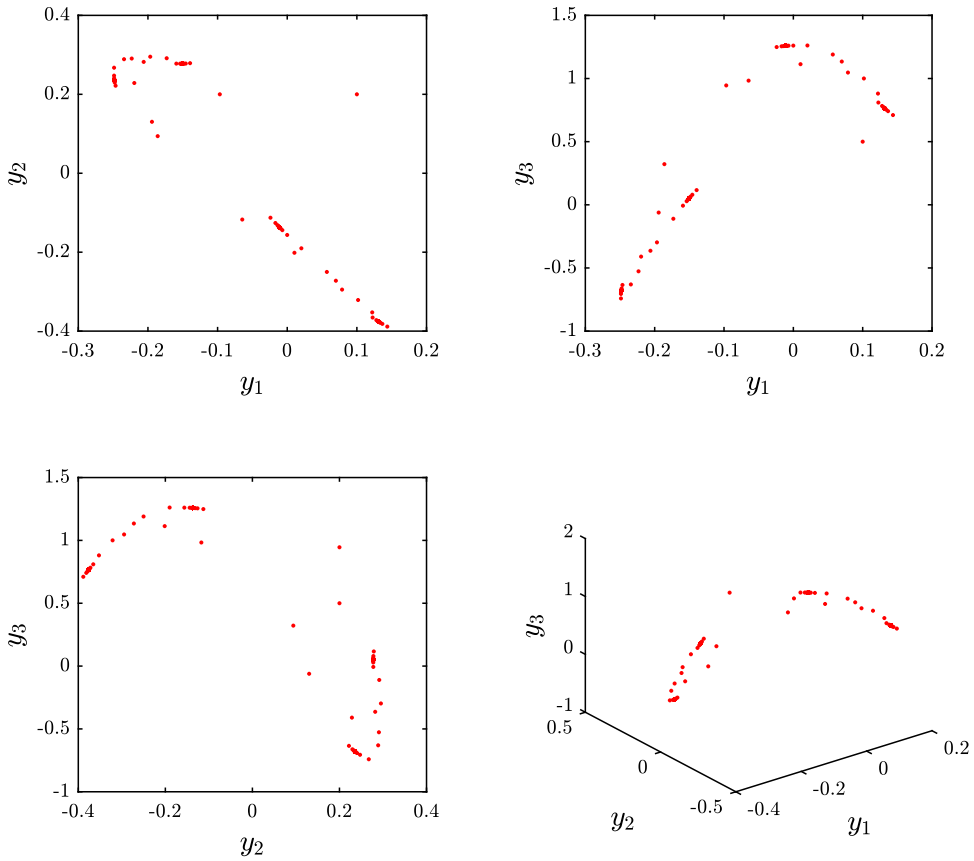

Figure 5. Phase portraits for the hyperchaotic Hénon map with $(a_2,\ b_2) = (0.99,\ 0.2)$, $\beta = 0.984$ and $(y_1(0),\ y_2(0),\ y_3(0)) = (0.1, 0.2, 0.5)$.

$$\hat{\gamma} = \begin{pmatrix} 2 & 0 \\ 0 & 3 \end{pmatrix} \tag{38}$$

and make sure it is invertible, which it clearly is. Its inverse is simply given by

$$\hat{\gamma}^{-1} = \begin{pmatrix} 1/2 & 0 \\ 0 & 1/3 \end{pmatrix}. \tag{39}$$

According to Theorem 3, there exists a control matrix L such that the eigenvalues of $(\hat{B} - L)$ satisfy (31). We simply choose

$$L = \begin{pmatrix} 0 & 9/16 \\ 0 & -3/2 \end{pmatrix}, \tag{40}$$

leading to

$$\hat{B} - L = \begin{pmatrix} -1 & -9/16 \\ 1 & 1/2 \end{pmatrix}. \tag{41}$$

It is easy to see that all the eigenvalues of $\hat{B} - L$ satisfy condition (31). All that remains is to calculate matrix R according to (27), vector $\hat{U}$ according to (28), and append it with a zero at the end as specified in (25). The resulting synchronisation error system is of the form

$$\begin{cases} {}^{\mathrm{C}}\Delta^{\beta} e_1(t) = -e_1(t+\beta-1) - \dfrac{9}{16} e_2(t+\beta-1), \\ {}^{\mathrm{C}}\Delta^{\beta} e_2(t) = e_1(t+\beta-1) + \dfrac{1}{2} e_2(t+\beta-1). \end{cases} \tag{42}$$

Given the initial errors $(e_1(0), e_2(0)) = (-1, -2)$, figure 6 depicts the time evolution of the errors (42). The errors clearly converge towards the zero solution in sufficient time indicating successful synchronisation between the master and the slave maps. The computational complexity involved in the calculation of R according to (27) and then $\hat{U}$ according to (28) can be shown to be $m^2 + 2n^2 + 4nm = 41$ MAC operations per iteration.

4. Discussion

Now that we have presented the analytical findings and illustrated them with numerical simulations, let us highlight the novelty introduced by the presented approach. First of all, we note that to the best of the knowledge of the authors, the results reported in the literature on the synchronisation of hybrid systems are solely

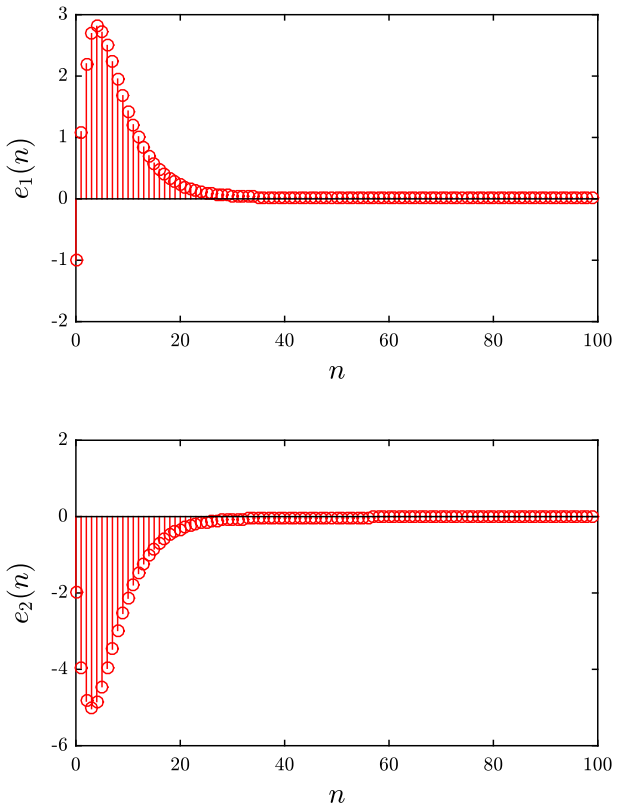

Figure 6. The evolution of errors over time for the first example as in (42).

dedicated to continuous-time differential systems. The topic related to the synchronisation of integer-order and fractional-order discrete-time systems is completely unexplored.

In this work, synchronisation has been guaranteed in different dimensions by using two approaches: the integer-order Lyapunov stability method in discrete-time and the stability theory of linear fractional-order discrete-time systems. The achieved controller is proposed in the general case and may be applied to non-identical chaotic maps of different dimensions. In addition, the proposed FSHPS and IFSHPS synchronisation schemes can be considered as a generalisation of many existing schemes such as complete synchronisation, anti-synchronisation, projective synchronisation and hybrid synchronisation. It is our opinion that the proposed controllers are suitable for the cases where the controlled hybrid systems exhibit chaotic behaviours. However, in real world, periodical synchronisation may be more practical to synchronise arbitrary hybrid systems.

Based on the previous considerations, it should be clear that the methods proposed herein provide a contribution to the topic related to the synchronisation between integer-order and fractional-order discrete-time systems. This increased complexity is related simultaneously to the synchronisation types and the capability to synchronise chaotic dynamics with hyperchaotic ones as well as providing a deeper insight into the synchronisation phenomena between hybrid systems described by integer-order and fractional-order discrete-time systems with different dimensions.

5. Conclusion

In this paper, we examined the synchronisation of different types of discrete-time chaotic systems. We proposed an adaptive control strategy to achieve FSHPS between a fractional-order master and an integer-order slave maps. The asymptotic convergence of the synchronisation errors to zero is proved by means of the conventional integer-order direct Lyapunov method. We have also presented an IFSHPS synchronisation scheme for an integer-order master and a fractional-order slave maps. The convergence of the second controller is guaranteed by means of the stability theory of linear fractional discrete-time systems. Two numerical examples were presented to illustrate the findings by taking into consideration the standard Hénon map, the fractional Hénon map, the generalised Hénon map and the fractional generalised Hénon map. Simulation results show that the proposed control laws are valid and that the synchronisation error converges towards zero over time.

Acknowledgements

The authors acknowledge Prof. GuanRong Chen, Department of Electronic Engineering, City University of Hong Kong for suggesting many helpful references.

References

[1] L M Pecora and T L Carrol, *Phys. Rev. Lett.* **64**, 821 (1990)
[2] L Kocarev and S Lian, *Chaos-based cryptography: Theory, algorithms and applications* (Springer-Verlag, Berlin, Heidelberg, 2011)
[3] K M Cuomo, A V Oppenheim and S H Strogatz, *Int. J. Bifurc. Chaos* **3**, 1629 (1993)
[4] G Millerioux and J Daafouz, *Int. J. Bifurc. Chaos* **14**, 1357 (2004)
[5] H Dedieu, M P Kennedy and M Hasler, *IEEE Trans. Circuits Syst. II: Analog Digital Signal Process.* **40**, 634 (1993)
[6] K K Tse, R Wai-Man Ng, H S Chung and S Y Ron Hui, *IEEE Trans. Ind. Electron.* **50**, 171 (2003)

[7] D He and H Leung, *IEEE Trans. Circuits Syst. II: Express Briefs* **52**, 739 (2005)
[8] R Liang, X Tan, H Zhou and S Wang, *Pramana – J. Phys.* **85**, 617 (2015)
[9] T Yang and L Chua, *IEEE Trans. Circuits Syst. I* **44**, 976 (1997)
[10] M Hénon, *Commun. Math. Phys.* **50**, 69 (1976)
[11] R Lozi, *J. Phys.* **39**, 9 (1978)
[12] D L Hitzl and F Zele, *Physica D* **14**, 305 (1985)
[13] G Baier and S Sahle, *Phys. Rev. E* **51**, 2712 (1995)
[14] A Ouannas, A T Azar and R Abu-Saris, *Int. J. Mach. Learn. Cyber.* **8**, 1887 (2017)
[15] A Ouannas and G Grassi, *Nonlinear Dyn.* **86**, 1319 (2016)
[16] A Ouannas and Z Odibat, *Nonlinear Dyn.* **81**, 765 (2015)
[17] A Ouannas, *J. Comput. Nonlinear Dyn.* **10**, 061019 (2015)
[18] A Ouannas and G Grassi, *Chin. Phys. B* **25**, 090503 (2016)
[19] A Ouannas, G Grassi, A Karouma, T Ziar, X Wang and V-T Pham, *Open Phys.* **16**, 174 (2018)
[20] F Wu, P Zhou, A Alsaedi, T Hayat and J Ma, *Chaos Solitons Fractals* **110**, 124 (2018)
[21] F M Atici and P W Eloe, *Electron. J. Qual. Theory Differ. Equ. Spec. Ed. I* **3**, 1 (2009)
[22] T Abdeljawad, *Comput. Math. Appl.* **62**, 1602 (2011)
[23] T Abdeljawad, D Baleanu, F Jarad and R P Agarwal, *Discret. Dyn. Nat. Soc.* **2013**, 104173 (2013)
[24] D Baleanu, G Wu, Y Bai and F Chen, *Commun. Nonlinear Sci. Numer. Simul.* **48**, 520 (2017)
[25] C Goodrich and A C Peterson, *Discrete fractional calculus* (Springer, Switzerland, 2015)
[26] T Hu, *Appl. Math.* **5**, 2243 (2014)
[27] M K Shukla and B B Sharma, *Int. J. Electron. Commun.* **78**, 265 (2017)
[28] A Deshpande and V Daftardar-Gejji, *Pramana – J. Phys.* **87**: 49 (2016)
[29] G Wu and D Baleanu, *Signal Process.* **102**, 96 (2014)
[30] G Wu, D Baleanu, H Xie and F Chen, *Physica A* **460**, 374 (2016)
[31] Y Liu, *Indian J. Phys.* **90**, 313 (2016)
[32] S Kassim, H Hamiche, S Djennoune and M Bettayeb, *Nonlinear Dyn.* **88**, 2473 (2017)
[33] O Megherbi, H Hamiche, S Djennoune and M Bettayeb, *Nonlinear Dyn.* **90**, 1519 (2017)
[34] B Xin, L Liu, G Hou and Y Ma, *Entropy* **19**, 351 (2017)
[35] A Ouannas, X Wang, V T Pham and T Ziar, *Complexity* **2017**, 4948392 (2017)
[36] A Ouannas, O Zehrour and Z Laadjal, *Nonlinear Studies* **25**, 91 (2018)
[37] A Ouannas, *J. Nonlinear Dyn.* **2014**, 983293 (2014)
[38] C Wang, R Chu and J Ma, *Complexity* **21**, 370 (2015)
[39] J Cermak, I Gyori and L Nechvatal, *Fract. Calc. Appl. Anal.* **18**, 651 (2015)